How To Design for a Tailored Subcellular Distribution of Systemic Agrochemicals in Plant Tissues

Hofstetter, Sandro; Beck, Andreas; Trapp, Stefan; Buchholz, Anke

Published in:
Journal of Agricultural and Food Chemistry

Link to article, DOI:
10.1021/acs.jafc.8b02221

Publication date:
2018

Document Version
Peer reviewed version

How to design for a tailored subcellular distribution of systemic agrochemicals in plant tissues

Sandro Hofstetter (1), Andreas Beck (1), Stefan Trapp (2), Anke Buchholz (1,*)

[1] Syngenta Crop Protection AG, Schaffhauserstrasse 101, 4332 Stein, Switzerland

[2] Technical University of Denmark, Miljoevej 113, 2800 Kongens Lyngby, Denmark

* anke.buchholz@syngenta.com, Tel +41 62 866 0145, Fax +41 62 866 0864

Running title: Predicting intracellular localization of agrochemicals in plant tissues

Abstract

Foliar applied systemic agrochemicals require the entrance into the plant vascular system or into specific subcellular compartments to reach their target in planta or to be imbibed by piercing-sucking pests. An inappropriate subcellular localization, like accumulation of aphicides in vacuoles, might lower compound efficiency due to reduced exposure to the target.

Permeabilities and mass distributions of sixteen compounds covering a broad range of properties were measured across a pH gradient in a PAMPA ('Parallel artificial membrane permeability assay') system, providing experimental evidence for ion trapping of acids and bases in basic and acidic compartments, respectively. The results validated a predictive model which was then expanded to simulate a standardized plant cell (cytosol and vacuole) with vascular system (phloem and xylem).

This approach underlined that the absolute mass distribution across aqueous phases was defined by membrane retention (M_r) whereas the relative mass distribution was determined by the species (neutral, acidic, basic) of compounds. These processes depend largely on pK_a and log K_{ow} of the test compounds, which subsequently determine the partitioning of the substances in plant cell compartments. The validated model can be used as a tool in agrochemistry research to tailor the subcellular distribution by chemistry design and to interpret biology results.

Keywords:

PAMPA, intracellular localization model, pH partition hypothesis, vacuole trapping

Introduction

Eukaryotic cells have highly organized subcellular compartments with distinct structural and functional features. Plant vacuoles are versatile organelles with a crucial role in osmoregulation, undertaking functions such as recycling, detoxification and storage [14]. Different transport processes occur at the vacuolar membrane for inorganic or biotic solutes [30]. The electrochemical and pH gradient generated by channels and transporters might also lead to an accumulation of xenobiotics within this largest cell compartment of mature plant cells.

The present study aims to provide experimental evidence for the postulated vacuole trapping of basic pesticides in leaf cells [10, 11, 34].

The accumulation of weakly basic compounds in acidic organelles has been observed in animal and human cells [12, 17, 46, 51] and was also recently discovered for acidic vesicles of protozoa [20]. Ion trapping of weakly acidic herbicides leads to phloem transport and systemic translocation in plants [27, 48] and is well described for phytohormones such as auxins [21, 35] and abscisic acid [23]. It is expected that a similar passive mechanism occurs in plant cells, whereby weakly basic compounds are distributed into the large acidic vacuoles. The passive accumulation of alkaloids in acidic latex vacuoles against a concentration gradient was described by Hauser and Wink (1990) [24]. On the macroscale, an increased accumulation of weak bases in plants was observed with increasing pH [25, 36]. But as of yet, no systematic study on the ion trap effect due to pH gradients of weakly alkaline pesticides has been published.

Calculations based on first principles indicated that intrinsically very active pesticides might not show sufficient translaminar pest control which is required for a robust field performance against sucking pests after foliar spray if trapping in vacuoles inhibits dose

effective translaminar distribution [8]. Especially phloem feeders such as aphids and whiteflies avoid piercing their stylet into the vacuole which contains natural plant defense compounds like alkaloids [22]. Lipophilic compounds may be limited in translaminar diffusive transport, as they stick to membranes and other lipophilic structures [8]. On the other hand, partitioning into membranes favors membrane permeation and thus symplastic transport inside mesophyll cells. Compounds accumulating inside of cells could be imbibed by cell feeders like thrips and mites. The design for specific intracellular distribution profiles may thus be seen as a new approach for target selectivity of pesticides [7].

Initially we will provide experimental evidence for ion trapping of acids and bases in basic and acidic compartments, respectively. This was done by determining the permeabilities and mass distributions of diverse agrochemicals across a pH gradient between two differentially adjusted compartments in a 'Parallel artificial membrane permeability assay' (PAMPA). The permeabilities were measured in a kinetic and equilibrium approach.

In a second step we will compare the measured mass fractions with the postulated distributions as calculated with a cell model [50, 51]. This model is gradually expanded to a four compartment model representing a standardized plant cell (cytosol and vacuole) and plant vascular system (phloem and xylem).

This paper provides results on a broad range of chemistry and also validates a model that allows to interpret and to predict intracellular localization. This knowledge on subcellular localization of new active ingredients in plant cells can be exploited for selective targeting of pests and is an essential element in research of modern agrochemistry.

Material and Methods

Reagents. Sixteen compounds comprising monoprotic weak acids, monoprotic weak bases and neutral compounds and differing in acid dissociation (pK_a) and lipophilicity were selected for the experiments. This set of compounds included diverse chemistries including commercial agrochemicals, research compounds and the reference drug carbamazepine. The commercial insecticides pymetrozine (PYME), thiamethoxam (THMX), cyantraniliprole (CYNT), spirotetramat (SPAT) and its free acid, spirotetramat enol (SPAT enol) as well as the research compounds oxazoline (OX), imidazoline (IM) and additional research compounds (compd 1 to compd 8), which were synthesized in house. Carbamazepine (CBZ), DMSO (analytical grade), formic acid, acetonitrile (HPLC grade), methanol (HPLC grade) were obtained from Sigma-Aldrich (St Louis, MO).

The chemical structures of the compounds are shown in Figure 1. The name, abbreviation, molecular weight, pK_a, log K_{ow} as well as log D (calculated) of test compounds are shown in Table 1. Physicochemical properties were either taken from literature or measured/calculated in-house. All weak bases had a pK_a well above 7.0 whereas the weak acids possessed a pK_a well below 5.5. The log K_{ow} ranged from -0.2 to 6.8.

The water used in this study was purified (> 18 MΩ cm) with Milli-Q Advantage A10 from Millipore (Merck KGaA, Darmstadt, Germany).

Parallel artificial membrane permeability assay (PAMPA). PAMPA evaluation software (PAMPA Explorer version 3.7.2) and Gutbox^{TM} were used from Pion (Billerica, MA). Donor plates (Multiscreen Transport Receiver Plate, MATRNPS50), acceptor plates (Multiscreen-IP, MAIPN4550, pore size 0.45 µm) and filtration plates (Multiscreen-HV, MSHVN4550, 0.45 µm pore size) were purchased from Millipore (Merck KGaA, Darmstadt, Germany). Flat bottom UV-plates (reference plate) were obtained from Thermo-Fisher (Waltham, MA). Dodecane

(reagentPlus), MES and HEPES buffer were acquired from Sigma Aldrich (St Louis, MO). L-α-phosphatidylcholine from egg yolk (ca. 60%; TLC grade) from Sigma Aldrich (St Louis, MO) was not further purified and stored at -20 °C prior to use. The phospholipid solution was prepared before usage as 10% (w/v) phosphatidylcholine in dodecane. All test compounds were prepared as 10'000 mg/L stock solution in DMSO. The test solutions were further diluted with 50 mM MES (pH 5.5) or HEPES buffer (pH 7.0) to 50 mg/L, keeping the final DMSO concentration below 1% (v/v) and filtered through a filtration plate (0.45 µm pores) prior to usage to ensure a homogenous solution.

PAMPA was performed in 96 well plates as described elsewhere [16, 32]. The PAMPA sandwich assembly contained a donor plate and an acceptor plate creating two chambers separated by a microfilter disc (Figure 2). The filter disc was coated with 5 µL of phospholipid solution and dried for 30 min. The Tecan freedom EVO liquid handler transferred an aliquot from the test solutions into the donor plate and reference plate. The acceptor plate was prepared with acceptor buffer and the PAMPA sandwich was assembled together with the donor plate. Incubation occurred at room temperature under constant humidity in the Gut-Box™. The PAMPA sandwich was disassembled after incubation and an aliquot of both acceptor and donor solution was quantified. The compound distribution between donor, acceptor and the remaining fraction in the filter was compared to a reference sample which was directly measured after initiation of incubation.

Compounds in the permeability assay were measured under a bidirectional pH sink condition, initially having pH 7.0 in the acceptor plate and pH 5.5 in the donor plate, and following these measurements the pH gradients was reversed. These pH values were chosen to mimic an ideal plant cell simplified to two equally sized compartments, the cytosol (pH 7.0) and the embedded vacuole (pH 5.5). This gradient is more pronounced than

common applications in pharma where the blood (pH 7.4) and small intestine (pH 6.5) are mimicked [26]. A test series generally contained DMSO as a blank and carbamazepine as an internal reference standard. Compounds were measured in triplicates in each run.

Kinetic approach. The permeability of the compounds was tested across a pH gradient from pH 7.0 to pH 5.5 and *vice versa*. The assay was done without any additional sink condition in the acceptor compartment (e.g. sodium dodecyl sulfate [1]) and performed without stirring [3]. The majority of investigated compounds displayed moderate hydrophobicity, i.e. log D (pH 5.5 / 7.0) ≤ 2.5, supposing unaffected permeability through the membrane (except compd 1, 2, 7 and 8). Inside living cells the cytosol streaming would largely eliminate unstirred boundary layers, whereas in the PAMPA system unstirred boundary layers may provide additional resistance. However, the effect of the unstirred boundary layer is minor compared to the resistance of the artificial membrane layer with a thickness of 125 µm [2], except for the highly lipophilic compounds [9].

In the kinetic approach, the incubation time was 18 h and quantification was performed by UV spectrum (230 - 500 nm) analysis. The effective permeability (P_e) was measured by UV/Vis spectra (TECAN® infinite M200pro) and evaluated with the PAMPA evaluation software (PAMPA Explorer, Pion) [29].

Equilibrium approach. In this thermodynamic approach (phase equilibrium condition), the PAMPA sandwich was incubated for six days without stirring. After this incubation period, the mass fractions in the donor and acceptor compartment were measured by UPLC (ultra-performance liquid chromatography) mass spectrometer. All other conditions were identical to the kinetic approach. During this time it is expected that equilibrium is established due to

143 the small size of the system (600 µL). Equilibrium for neutral compounds means identical
144 concentrations in the donor and acceptor compartment, whereas higher concentrations are
145 expected in the alkaline and the acidic compartment for weak acids and weak bases,
146 respectively.
147 Compound concentrations were determined by UPLC-MS/UV. The UV/MS (ultraviolet / mass
148 spectrum) signal was recorded with Agilent 1200 UPLC system (Agilent Technologies, Santa
149 Clara, CA) equipped with an Acquity UPLC BEH C18 (2.1 x 50 mm, 1.7 µm) column at 60 °C
150 (Table S1). The mobile phase consisted of (A) HPLC grade water with 0.5% methanol and
151 0.05% formic acid and (B) acetonitrile with 0.05% formic acid. The elution started with a
152 mobile phase of 95% A for 12 s followed by a linear gradient to 100% B over 72 s. The mobile
153 phase was then changed gradually to 70% B for 40 s and returned to 5% B in the end. Peak
154 finding and peak area quantification was performed by using XCalibur 3.0 software (Thermo
155 Fischer Scientific).
156
157 **Mass distributions across donor and acceptor compartment.** Compartments could be either
158 considered as a real biological cell compartments (an aqueous phase surrounded by a
159 membrane) or as the bioavailability determining compartment (restriction to the aqueous
160 phase). The latter is the case if the aqueous phase reflects the dose limiting factor to control
161 e.g. sucking pests.
162 If donor and acceptor are considered as a biological cell compartment, the membrane
163 retention (M_r) is included in each phase. Masses in donor (M_d) and acceptor (M_a) were
164 quantified and the membrane retention (M_r) was derived by the mass balance; whereas
165 (M_{ref}) was the total mass in the reference plate:
166

$$M_r = M_{ref} - M_d - M_a \quad (1)$$

The mass fraction of donor (%M_d) was calculated as follows (Table S2):

$$\%M_d = 100 \times \frac{M_d}{(M_d+M_a+M_r)} \quad (2)$$

Mass fractions for acceptor (%M_a) and membrane retention (%M_r) were calculated accordingly.

If donor and acceptor compartments were restricted to their aqueous phase, the mass fraction of e.g. donor (%$M_{d,aq}$) was calculated neglecting the membrane retention:

$$\%M_{d,aq} = 100 \times \frac{M_d}{M_d+M_a} \quad (3)$$

Permeability with ion trapping conditions and related calculation of mass fractions. Weak acids and bases have two relevant molecule species that diffuse in the system, namely the neutral and the ionic species. The movement of ionized molecules across charged membranes is described by the Nernst-Planck equation [48], when the electrical potential approaches zero, the equation converges to Fick's Law of diffusion. In living cells, the ATPase creates a resting potential of about -100 mV at the outer membrane. Artificial systems with phosphatidylcholine membranes (PAMPA) have no ATPase. A small net charge can theoretically be generated due to the diffusion of buffers and electrolytic test compounds across the membrane (Goldman-Hodgkin-Katz-equation[19, 45]) but we do not expect this to

have a significant effect. We therefore neglect electrical charge at the membranes and calculate with Fick's 1st Law of diffusion. Accordingly, the overall exchange across the membrane is the net exchange of both molecule species:

$$\frac{dm}{dt} = A\,P_n(a_{n,d} - a_{n,a}) + A\,P_i(a_{i,d} - a_{i,a}) = A\,P_{e,da}C_d - A\,P_{e,ad}C_a \quad (4)$$

dm/dt is the exchange of chemical mass from donor to acceptor, A is the exchange area (membrane cross-area, cm^2), P (cm/s) is permeability (of n neutral species and i ion) and a is chemical activity in the donor (d) and acceptor (a) compartment. P_e is the effective permeability, composed of the permeability of the neutral and of the ionic species, from donor to acceptor (subscript da) or from acceptor to donor (subscript ad) compartment. For dilute aqueous solutions, activity a is approximately the same as concentration C in solution. The effective permeability P_e depends on the individual permeabilities of the neutral or the ionic species at a given pH. In case of steady-state, the ratio between concentrations of both compartments corresponds to the ratio of effective permeabilities. For equal volumes of donor and acceptor compartment, the concentration ratio is identical to the mass ratio, and Equation 5 follows Krämer (2016) [28]:

$$\frac{M_{a,Eq}}{M_{d,Eq}} = \frac{P_{e,da}}{P_{e,ad}} \quad (5)$$

The charged species has a membrane permeability which is orders of magnitude slower than the neutral species [49]. Therefore, the solute is trapped in the compartment where the

molecule is ionized, i.e., acids at higher pH and bases at lower pH [51]. In general, ion trapping only reduces P_e in the direction from the compartment with trapping to the one without [28]. In the absence of other diffusive processes, this mass ratio in steady-state equals the thermodynamic phase equilibrium, i.e. the endpoint of diffusion which is the system state with the highest entropy. Therefore, we determined P_e under both trapping conditions as forward permeability ($P_{e,fw}$) from pH 7.0 to pH 5.5 and as reverse permeability ($P_{e,rv}$) at steady state (i.e. determined after 18 h) (Equation 6 and 7):

$$donor\ (pH\ 7.0) \xrightarrow{P_e(fw)} acceptor(pH\ 5.5) \quad (6)$$

$$donor\ (pH\ 5.5) \xrightarrow{P_e(rv)} acceptor(pH\ 7.0) \quad (7)$$

The real mass fractions in donor and acceptor compartment (i.e. in aqueous phases) at equilibrium ($\%M_{a,eq}$ and $\%M_{d,eq}$) are obtained by considering the membrane retention ($\%M_r$) and reflecting the different directions of permeabilities ($P_{e,fw}$ and $P_{e,rv}$); as shown in Equation 8 and 9.

$$\%M_{a,eq} = (100 - \%M_r) \times \frac{P_{e,fw}}{P_{e,fw} + P_{e,rv}} \quad (8)$$

$$\%M_{d,eq} = (100 - \%M_r) \times \frac{P_{e,rv}}{P_{e,fw} + P_{e,rv}} \quad (9)$$

Accordingly, our calculations for the relative mass distribution in donor and acceptor at equilibrium were done with the membrane retention as measured in the equilibrium

231 approach and with the forward and reverse permeability as measured in the kinetic
232 approach.
233
234 **Cell model and adaptations.** The cell model has been used for a number of applications in
235 medicine [46, 50, 51], and it was also coupled to transport models of pesticides in plants [8, 47].
236 Here, we test and apply its core element, the model for intracellular distribution [48]. The
237 chemical input parameters, log K_{ow} neutral, log K_{ow} ion, pK_a, MW and the valency (charge
238 number) are shown in Table 1. The valency is +1 for bases (OX, IM and compd 3 to compd 8)
239 and -1 for acids (SPAT enol, compd 1 and compd 2).
240 The cell model parameters were adapted to reflect the conditions in our PAMPA test system
241 (Table S3): Only two compartments were considered (donor and acceptor). The volume of
242 the donor (= cytosol) and the acceptor (= vacuole) were equally sized with a total volume of
243 600 µL. The applied L-α-phosphatidylcholine concentration defined the lipid to water ratio as
244 0.83% to 99.17%. The membrane potential was set to 0.01 V. Equilibration started from the
245 cytosol (donor) and the mass distribution in the cytosol and vacuole were calculated for
246 $t = \infty$ after incubation start. The membrane retention represented the sum of both lipid
247 fractions of both compartments, plasmalemma (cytosol) and tonoplast (vacuole).
248
249 **Extension of the cell model to the four compartment model for plant tissues.** A predictive
250 model for localization of pesticides in cell compartments and transfer in plant tissues has
251 been described recently [8]. Thus far, the measured or predicted mass fractions in the 'PAMPA
252 cell model' cannot be directly translated to an *in planta* environment. For a direct
253 comparison the relative dimensions of different compartments and thickness (i.e. thinner) of
254 the biomembrane would have to be considered. These respective parameters are listed in

255 Table S3. This model includes besides both major cell compartments, the cytosol (pH 7.2)
256 and the vacuole (pH 5.5), but also both elements of the plant vascular system, the xylem (pH
257 5.5) and phloem (pH 8.0). This model approach only considered the cytosol and the vacuole
258 as compartments containing a lipid fraction, i.e. being surrounded by the plasmalemma and
259 tonoplast. Compounds in the lipid phase ('at lipids' fraction) or dissolved in the aqueous
260 phase ('solved' fraction) were therefore calculated separately for each cell compartment,
261 whereas the mass fraction in the xylem and phloem were exclusively described as the solved
262 fraction.
263
264 **Results**
265 **Kinetic measurements.** The permeability measurements were done under steady state
266 conditions (i.e. at constant kinetics) and indicated the preferred permeation direction with
267 different pH gradient conditions. Neutral compounds exhibited equal permeabilities (P_e) in
268 both pH gradient directions (Figure 3) within a range of 0.19 (± 0.01) × 10^{-6} to 11.45 (± 1.05)
269 × 10^{-6} cm/s (Table 2). The permeation of acidic compounds from pH 5.5 to pH 7.0 was in
270 average 40 times faster than in the opposite direction. All basic compounds permeated
271 faster from pH 7.0 to pH 5.5 by about factor 40; except for compd 3 which had similar
272 permeability in both pH gradients. Compd 3 is the most hydrophilic compound with a log D
273 of -3.6 at pH 5.5. Surprisingly it demonstrated very low permeability, close to the minimal
274 detection limit in both pH gradient directions. Previous investigations on other basic
275 hydrophilic compounds with bidirectional low permeabilites, proposed that ion-pair
276 mediated transport may explain this observation [42-44]. The permeability of the very lipophilic
277 compd 7 and compd 8 could not be measured.
278

279 **Verification of measurements using the pH-partition hypothesis.** Before further data
280 analysis, we had to exclude that exceptional anomalies of ionized species had affected our
281 permeability measurements. Experimental deviation could derive e.g. from an unstirred
282 aqueous boundary layer effect. Smolen (1973) [41] demonstrated that pH and pK_a showed the
283 same relationship as log D. Therefore we plotted the difference in log D between acidic and
284 basic compartment (Δ log D) and the difference of log P_e from pH 5.5 to pH 7.0 and *vice*
285 *versa* (Δ log P_e). The comparative fit with the ideal line (slope of -1 and the intercept is at
286 zero) would validate the concept of pH partitioning across the membrane (Figure 4).
287 SPAT enol, as an example, demonstrated a log P_e of -5.9 (direction pH 5.5 to pH 7.0) and
288 log P_e of -7.4 (direction pH 7.0 to pH 5.5) resulting in a Δ log P_e of 1.5. The corresponding Δ
289 log D was 1.5 with a log D of 1.7 (pH 5.5) and 0.4 (pH 7.0) in the donor and acceptor
290 compartment. Typically, neutral compounds exhibited no difference in log D in buffer
291 solutions with pH 7.0 or pH 5.5, resulting in no difference in log P_e. In contrary, most acids
292 and bases were confronted with a Δ log D of about 1.5 which was reflected in a Δ log P_e of
293 1.5 units.
294 Despite similar pKa as the other basic compounds, compound 3 behaved different and
295 showed similar permeabilities in both directions. This is likely due to an ion pairing
296 mechanism which allows ion pairs to cross membranes uncharged and thus as fast as the
297 neutral species.
298 Overall, we can state that the measured permeabilities of most test compounds were in
299 good alignment with the pH partitioning hypothesis (Smolen 1973), which also means that
300 the permeability of ions did not significantly contribute to the overall membrane
301 permeability.
302

Equilibrium measurements. The neutral compounds, CYNT and SPAT, exhibited equal distribution (50:50) between donor and acceptor for both pH gradient directions indicating complete equilibration (Figure 5). The polar neutral compounds, PYME and THMX, showed an unequal mass balance after six days favoring the donor compartment, independent of the pH gradient direction. The acidic compounds, compd 1 and compd 2, were almost entirely found in the neutral compartment as reflected by the very low fractions in the acidic compartment. However, for the third acid, SPAT enol, 61% remained in the acidic compartment (Table 2) if the equilibration started from an acidic donor. Most basic compounds (OX, compd 4, compd 6, IM and compd 7) almost exclusively remained in the acidic compartment demonstrating ion trapping irrespective of the direction of the pH gradient. Exceptions were compd 3 (postulated ion pairing, see above), compd 5 and compd 8.

Compounds stated as not equilibrated in Table 2 showed an unexpectedly high donor fraction as e.g. for PYME and THMX. Their very low permeabilities of ca. 0.2×10^{-6} cm/s (PYME) and ca. 0.7×10^{-6} cm/s (THMX) indicate a very slow equilibration. Very low permeability was also observed for the acid SPAT enol ($(1.30 \pm 0.03) \times 10^{-6}$ cm/s from pH 5.5 to pH 7.0) and for the base compd 3 ($(0.06 \pm 0.01) \times 10^{-6}$ cm/s from pH 7.0 to pH 5.5). These non-equilibrated compounds had a particularly low log D (Table 1).

A considerable amount of compd 5 remained in the neutral donor, when equilibrating from pH 7.0 to pH 5.5, which cannot be explained by a low permeability. The permeability of compd 5, $(8.54 \pm 0.94) \times 10^{-6}$ cm/s, was in the range of other basic compounds as for instance compd 4 with $(9.58 \pm 0.48) \times 10^{-6}$ cm/s and compd 6 with $(9.55 \pm 0.82) \times 10^{-6}$ cm/s.

Almost full membrane retention was measured for compd 8 which is obviously related to its high log K_{ow} of about 6.5 (Table 2). The equilibration from pH 7.0 to pH 5.5 was below the

detection limit for compd 8, suggesting major compound loss during the filtration step because of precipitation.

In general, the membrane retention at equilibrium was log K_{ow} dependent showing an increasing membrane fraction with increasing log K_{ow}. Assuming that measured permeabilities and equilibrated mass distributions are directly related to the physicochemical properties of tested compounds, the outcomes should be predictable with the mathematical cell model (see Methods).

Adapted cell model predicting compound equilibration in PAMPA test system. The experimental dimension of our applied PAMPA setup had to be reflected in the cell model. In principal, the model adaptations included the equal volume of donor and acceptor, the applied pH conditions and a modified lipid - water distribution (Table S3). The input parameters, acid dissociation constant, lipophilicity and valency are given for each compound in Table 1.

This 'PAMPA cell model' predicted an accumulation of basic compounds in the vacuole, accumulation of acidic compounds in the cytosol and equilibration for neutral compounds (Figure 6 A). Increasing membrane retention was described in correspondence to increasing log K_{ow} of test compounds.

The model predictions were compared with the mass distribution at equilibrium ($\%M_{a,eq}$ and $\%M_{d,eq}$), which could have been taken directly from the equilibrium measurements (Table 2). Since five compounds did not equilibrate within six days, the mass distribution at equilibrium was derived from their measured permeabilities (Equation 8). To be consistent, this extrapolation was done for all sixteen compounds (Figure 6 B).

350 The lack of membrane retention was correctly predicted for THMX and PYME, whereas the
351 lipid phase for the other neutral compounds was overestimated by factors of up to 1.8 (CBZ).
352 The membrane retention was correctly predicted for acids apart from a slight
353 overestimation for compd 2. The discrepancy between predicted and measured membrane
354 retention was generally low except for the lipophilic IM. The full membrane retention for
355 compd 7 and compd 8 was correctly predicted.
356 Predictions for the mass fraction in donor and acceptor were within a range of about 10%
357 deviation (if overestimated lipid fraction is corrected). The only outlier was compd 3 where
358 the measured mass balance did not fit with the prediction (probably due to postulated ion-
359 pairing).
360
361 **Predicting compound distribution within a four compartment model of plant tissues**. After
362 this validation of the cell model (Figure 6) and as a core element of the 'four compartment
363 model' the calculation of mass fractions can be extrapolated to an *in planta* environment.
364 Table 3 summarizes the calculated mass fractions 'at lipids' of the vacuole and cytosol, and
365 the solved fractions of the aqueous phase of all four standardized tissue compartments.
366 These five fractions outline 100% of the mass balance.
367 This type of prediction impressively highlights PYME and THMX as excellent systemic
368 insecticides [15, 18], with low membrane retention and highest distribution in the xylem
369 compared to the other compounds. Acidic compounds are predicted to preferentially
370 distribute in the cytosol and basic phloem compartment (up to 40%). This 'phloem trapping'
371 is well described for phytohormones [23, 35] and herbicides [6]. Basic compounds with log K_{ow}<3
372 were predicted to accumulate in the large, acidic vacuole. This 'vacuole trapping' was
373 recently postulated for both basic insecticides, OX and IM [8, 34]. The vacuolar fraction was

374 drastically reduced with compounds having a log K_{ow}>3 by losing a considerable amount in
375 the membrane retention.
376 This dataset illustrates the mutual influence of log K_{ow} and pK_a on mass distributions. First,
377 the amount distributing in the aqueous phase was highly dependent on the log D. Generally,
378 increasing log K_{ow} increases membrane retention. However, a separate relationship was
379 observed for each compound species: compounds with a log K_{ow} of about 2.3 resulted in a
380 membrane retention of 92% (CBZ) as neutral, of 18% (SPAT enol) as acidic and of 1% (OX) as
381 basic species (Figure 7 A). Second, the distribution within the aqueous phases revealed a pK_a
382 dependent pattern. The predicted quantities solved in vacuoles in relation to the overall
383 solved fractions amounted to 84-85% for neutral compounds, 8-11% for acidic compounds
384 and 98-100% for basic compounds (Figure 7 B). This similarity in behavior of acids on the one
385 hand and of bases on the other hand is due to the quite similar pKa-values in each group
386 (Table 1).
387 Consequently, the absolute amount of a compound solved in one of the four compartments,
388 was dictated by the membrane retention. The relative distribution across the four aqueous
389 phases remains equal within each species of compounds (neutral, acidic, basic).
390
391 **Discussion**
392 In general, PAMPA is used to investigate kinetics of membrane permeation but not to
393 measure equilibrium. This is even more evident when sink conditions are applied to mimic
394 protein binding or blood flow [4]. However, in our context we wanted to simulate a
395 standardized plant cell within the leaf mesophyll and we therefore assumed comparable
396 protein levels in both compartments (i.e. neglecting protein binding). Our results obtained
397 with the PAMPA method cannot be directly transferred to the plant cell scenario since both

398 compartments, donor and acceptor, were of equal volume. In a plant cell the vacuole with
399 about 90% takes the majority of the size. Additionally, the membrane thickness in the
400 PAMPA system is given by the filter dimension carrying the phospholipids. This artificial
401 membrane has a thickness of 125 µm [2] and is therefore about 20'000 times thicker than a 5
402 to 10 nm thick biological lipid bilayer [40]. Accordingly, we would have expected the time
403 needed to reach equilibration within the PAMPA system would be much longer than for a
404 real biological system *in situ*. The relevance of thickness and lipid composition of biological
405 membranes on solute permeability was reviewed by Shinoda (2016) [38].
406
407 The ion trap of weak electrolytes in plants is well documented, but mostly on the macroscale
408 or organismal level. The first tests with pesticides were done by Briggs, Rigitano et al. (1987)
409 [5], where the authors demonstrated that with a series of (weakly acidic) phenoxy acetic acids,
410 both the uptake into barley roots and the translocation to shoots depended on the pH of the
411 external solution and increased with decreasing pH [5, 37]. Later, in a study with (weakly
412 alkaline) phenethylamines and anilines a similar effect but in the opposite direction was
413 demonstrated [25]. This is due to pH differences between external solution and plant cells. If a
414 chemical dissociates in the physiologically relevant range, this influences both uptake
415 velocity and volume. Rendal, Kusk et al. (2011) [36] reviewed 117 ecotoxicology results where
416 toxicity and bioaccumulation of weak acids or bases were tested at multiple pH levels.
417 Toxicity and bioconcentration factors (BCFs) increased for acids at lower pH, the opposite
418 was found for bases. The values of EC50 or BCF changed with pH when pH minus pK_a was in
419 the range of - 1 to 3 for acids, and - 3 to 1 for bases. According to the Henderson-Hasselbalch
420 equation, weak acids and bases occur in both neutral and ionic species in this range, and the

421 effect therefore can be attributed to a change of the ion trap effect. Interestingly single-
422 celled algae also show an effect of pH on toxicity of electrolytes [33].
423
424 Direct *in situ* measurements of the concentration in acidic vacuoles are difficult due to the
425 small size of these intracellular organelles. The authors originally attempted an experimental
426 validation on compound localization in vacuole suspensions isolated from barley [31].
427 However, the required separation steps starting from a protoplast suspension ended many
428 times with concentrations in vacuole fractions too close to the detection limits of test
429 compounds (unpublished results). A recent medical study succeeded in measuring
430 concentrations in lysosomes by using Raman scatter and found an accumulation of the weak
431 bivalent base chloroquine more than 1'000 fold [17]. Our results corroborate these findings.
432 Moreover, we obtained effective permeabilities, and the permeability ratios at varying pH
433 levels which are relevant for the distribution of compounds in the cytosol – vacuole system.
434 Our results are not on the intracellular scale, but mimic those conditions. They can thus be
435 considered as valid for the intracellular distribution in a plant cell. For this, practically no
436 measured concentration values are available. The experimental results of our adapted
437 PAMPA system and the model predictions are generally in very good alignment.
438 Discrepancies were seen for: very lipophilic compounds (that can be explained with the
439 experimental difficulties in detection of such compounds), compd 3 (postulated ion pairing)
440 and compd 5. We can thus use this PAMPA system to obtain data that can be transferred to
441 the intracellular level of plant leaves; and by the application of the model, we can scale-up
442 for the transversal transfer across leaves. This information is highly relevant for the design of
443 modern agrochemicals. Moreover, the consideration of intracellular distribution of
444 compounds is a new and additional way to optimize for more selective plant protection

445 products related to the mode of action and target of a given chemistry. The subcellular
446 distribution of small molecules and related cellular pharmacokinetics retain a great
447 importance in drug design [53].
448
449 The passive permeation of small solutes across lipid membranes is a fundamental process in
450 biology. The membrane permeability of compounds is correlated to their lipophilicity (log
451 K_{ow}). The log K_{ow} for drugs and agrochemicals is typically found below 5 [13]. Agrochemicals
452 show systemic behavior (i.e. long-distance translocation within xylem or phloem) with log
453 K_{ow} below 3 [39]. The mass distributions across plant cell compartments could be well
454 predicted for a broad range of agrochemicals using the presented and now validated model.
455 This makes reference measurements in a PAMPA system obsolete if exceptions in
456 membrane permeability (e.g. ion pairing) could be excluded. Provided that active transport
457 processes mediated through transporters or channels and metabolic transformation are
458 subordinated, the 'four compartment model' offers a great tool for chemistry design and
459 data analysis of biology results in optimization of new agrochemical chemistries.
460
461 **Supporting Information description**
462 The supplement provides the measured data of the equilibrium approach (Table S1), the
463 related calculations on mass fractions (Table S2) and all parameter data for the two
464 compartment model and the expanded four compartment model (Table S3).

References

1. Acosta, E., 3 - Testing the effectiveness of nutrient delivery systems. In *Delivery and Controlled Release of Bioactives in Foods and Nutraceuticals*, Garti, N., Ed. Woodhead Publishing: Cambridge, England, 2008; pp 53-106.
2. Assmus, F.; Ross, A.; Fischer, H.; Seelig, J.; Seelig, A., 31P and 1H NMR Studies of the Molecular Organization of Lipids in the Parallel Artificial Membrane Permeability Assay. *Mol. Pharm.* **2017,** *14* (1), 284-295.
3. Avdeef, A.; Bendels, S.; Di, L.; Faller, B.; Kansy, M.; Sugano, K.; Yamauchi, Y., PAMPA--critical factors for better predictions of absorption. *J. Pharm. Sci.* **2007,** *96* (11), 2893-2909.
4. Bermejo, M.; Avdeef, A.; Ruiz, A.; Nalda, R.; Ruell, J. A.; Tsinman, O.; Gonzalez, I.; Fernandez, C.; Sanchez, G.; Garrigues, T. M.; Merino, V., PAMPA--a drug absorption in vitro model 7. Comparing rat in situ, Caco-2, and PAMPA permeability of fluoroquinolones. *Eur. J. Pharm. Sci.* **2004,** *21* (4), 429-441.
5. Briggs, G. G.; Rigitano, R. L. O.; Bromilow, R. H., Physico-chemical factors affecting uptake by roots and translocation to shoots of weak acids in barley. *Pesticide Science* **1987,** *19* (2), 101-112.
6. Bromilow, R. H.; Chamberlain, K.; Evans, A. A., Physicochemical Aspects of Phloem Translocation of Herbicides. *Weed Science* **1990,** *38* (3), 305-314.
7. Buchholz, A.; O'Sullivan, A. C.; Trapp, S., What Makes a Good Compound against Sucking Pests? In *Discovery and Synthesis of Crop Protection Products*, American Chemical Society: Washington, DC, 2015; Vol. 1204, pp 93-109.
8. Buchholz, A.; Trapp, S., How active ingredient localisation in plant tissues determines the targeted pest spectrum of different chemistries. *Pest. Manag. Sci.* **2016,** *72* (5), 929-939.
9. Camenisch, G.; Folkers, G.; van de Waterbeemd, H., Review of theoretical passive drug absorption models: historical background, recent developments and limitations. *Pharm. Acta. Helv.* **1996,** *71* (5), 309-327.
10. Cassayre, J.; Hüter, O.; Hughes, D.; O'Sullivan, A.; Craig, W.; Jacob, O.; Clarke, E.; Earley, F.; Schade, A., Synthesis and Insecticidal Activity of New 2-Aryl-3,5-dihydro-2H-1,4-Benzoxazepine Derivatives. In *Discovery and Synthesis of Crop Protection Products*, American Chemical Society: Washington, DC, 2015; Vol. 1204, pp 391-410.
11. Creemer, L. C.; Giampietro, N. C.; Lambert, W.; Yap, M. C.; deBoer, G. J.; Adelfinskaya, Y.; Castetter, S.; Wessels, F. J., Pro-insecticidal approach towards increasing in planta activity. *Pest. Manag. Sci.* **2017,** *73* (4), 752-760.
12. De Duve, C.; De Barsy, T.; Poole, B.; Trouet, A.; Tulkens, P.; Van Hoof, F. o., Lysosomotropic agents. *Biochemical Pharmacology* **1974,** *23* (18), 2495-2531.
13. Delaney, J.; Clarke, E.; Hughes, D.; Rice, M., Modern agrochemical research: a missed opportunity for drug discovery? *Drug. Discov. Today* **2006,** *11* (17-18), 839-845.
14. Eisenach, C.; Francisco, R.; Martinoia, E., Plant vacuoles. *Curr. Biol.* **2015,** *25* (4), R136-R137.
15. Elbert, A.; Haas, M.; Springer, B.; Thielert, W.; Nauen, R., Applied aspects of neonicotinoid uses in crop protection. *Pest. Manag. Sci.* **2008,** *64* (11), 1099-1105.
16. Fischer, H.; Kansy, M.; Avdeef, A.; Senner, F., Permeation of permanently positive charged molecules through artificial membranes--influence of physico-chemical properties. *Eur. J. Pharm. Sci.* **2007,** *31* (1), 32-42.
17. Fu, D.; Zhou, J.; Zhu, W. S.; Manley, P. W.; Wang, Y. K.; Hood, T.; Wylie, A.; Xie, X. S., Imaging the intracellular distribution of tyrosine kinase inhibitors in living cells with quantitative hyperspectral stimulated Raman scattering. *Nat. Chem.* **2014,** *6* (7), 614-622.
18. Fuog, D.; Fergusson, S. J.; Flückiger, C., Pymetrozine: A Novel Insecticide Affecting Aphids and Whiteflies. In *Insecticides with Novel Modes of Action: Mechanisms and Application*, Ishaaya, I.; Degheele, D., Eds. Springer Berlin Heidelberg: Berlin, Heidelberg, 1998; pp 40-49.
19. Goldman, D. E., Potential, Impedance, and Rectification in Membranes. *The Journal of General Physiology* **1943,** *27* (1), 37-60.

20. Gulde, R.; Anliker, S.; Kohler, H. E.; Fenner, K., Ion Trapping of Amines in Protozoa: A Novel Removal Mechanism for Micropollutants in Activated Sludge. *Environ. Sci. Technol.* **2018,** *52* (1), 52-60.
21. Gutknecht, J.; Walter, A., Transport of auxin (indoleacetic acid) through lipid bilayer membranes. *J. Membr. Biol.* **1980,** *56* (1), 65-72.
22. Hartmann, T.; Ober, D., Biosynthesis and Metabolism of Pyrrolizidine Alkaloids in Plants and Specialized Insect Herbivores. In *Biosynthesis: Aromatic Polyketides, Isoprenoids, Alkaloids*, Leeper, F. J.; Vederas, J. C., Eds. Springer Berlin Heidelberg: Berlin, Heidelberg, 2000; pp 207-243.
23. Hartung, W.; Slovik, S., Physicochemical properties of plant growth regulators and plant tissues determine their distribution and redistribution: stomatal regulation by abscisic acid in leaves. *New Phytologist* **1991,** *119* (3), 361-382.
24. Hauser, M.-T.; Wink, M., Uptake of Alkaloids by Latex Vesicles and Isolated Mesophyll Vacuoles of Chelidonium ntajus (Papaveraceae). In *Zeitschrift für Naturforschung C*, 1990; Vol. 45, pp 949-957.
25. Inoue, J.; Chamberlain, K.; Bromilow, R. H., Physicochemical factors affecting the uptake by roots and translocation to shoots of amine bases in barley. *Pesticide Science* **1998,** *54* (1), 8-21.
26. Kansy, M.; Senner, F.; Gubernator, K., Physicochemical high throughput screening: parallel artificial membrane permeation assay in the description of passive absorption processes. *J. Med. Chem.* **1998,** *41* (7), 1007-1010.
27. Kleier, D. A., Phloem mobility of xenobiotics: I. Mathematical model unifying the weak Acid and intermediate permeability theories. *Plant. Physiol.* **1988,** *86* (3), 803-810.
28. Krämer, S. D., Quantitative aspects of drug permeation across in vitro and in vivo barriers. *Eur. J. Pharm. Sci.* **2016,** *87*, 30-46.
29. Lumbroso, A.; Villedieu-Percheron, E.; Zurwerra, D.; Screpanti, C.; Lachia, M.; Dakas, P. Y.; Castelli, L.; Paul, V.; Wolf, H. C.; Sayer, D.; Beck, A.; Rendine, S.; Fonne-Pfister, R.; De Mesmaeker, A., Simplified strigolactams as potent analogues of strigolactones for the seed germination induction of Orobanche cumana Wallr. *Pest. Manag. Sci.* **2016,** *72* (11), 2054-2068.
30. Martinoia, E.; Massonneau, A.; Frangne, N., Transport processes of solutes across the vacuolar membrane of higher plants. *Plant. Cell Physiol.* **2000,** *41* (11), 1175-1186.
31. Martinoia, E.; Schramm, M. J.; Kaiser, G.; Kaiser, W. M.; Heber, U., Transport of anions in isolated barley vacuoles : I. Permeability to anions and evidence for a cl-uptake system. *Plant Physiol.* **1986,** *80* (4), 895-901.
32. Muller, J.; Esso, K.; Dargo, G.; Konczol, A.; Balogh, G. T., Tuning the predictive capacity of the PAMPA-BBB model. *Eur. J. Pharm. Sci.* **2015,** *79*, 53-60.
33. Neuwoehner, J.; Escher, B. I., The pH-dependent toxicity of basic pharmaceuticals in the green algae Scenedesmus vacuolatus can be explained with a toxicokinetic ion-trapping model. *Aquat. Toxicol.* **2011,** *101* (1), 266-275.
34. O'Sullivan, A. C.; Schaetzer, J. H.; Luethy, C.; Mathews, C. J.; Elliott, C.; Pitterna, T.; Pabba, J.; Jacob, O.; Buchholz, A.; Blythe, J., Synthesis and Insecticidal Activity of New Benzyl- and Indanyl-Oxazolines, Thiazolines and Alkoxy-Alkyl-Imidazolines. In *Discovery and Synthesis of Crop Protection Products*, American Chemical Society: Washington, DC, 2015; Vol. 1204, pp 411-430.
35. Raven, J. A., Transport of Indoleacetic Acid in Plant Cells in Relation to pH and Electrical Potential Gradients, and its Significance for Polar IAA Transport. *New Phytologist* **1975,** *74* (2), 163-172.
36. Rendal, C.; Kusk, K. O.; Trapp, S., The effect of pH on the uptake and toxicity of the bivalent weak base chloroquine tested on Salix viminalis and Daphnia magna. *Environ. Toxicol. Chem.* **2011,** *30* (2), 354-359.
37. Rigitano, R. L. O.; Bromilow, R. H.; Briggs, G. G.; Chamberlain, K., Phloem translocation of weak acids in ricinus communis. *Pesticide Science* **1987,** *19* (2), 113-133.
38. Shinoda, W., Permeability across lipid membranes. *Biochimica et Biophysica Acta (BBA) - Biomembranes* **2016,** *1858* (10), 2254-2265.

39. Sicbaldi, F.; Attilio Sacchi, G.; Trevisan, M.; A. M. Del Re, A., *Root Uptake and Xylem Translocation of Pesticides from Different Chemical Classes*. 1997; Vol. 50, p 111-119.
40. Sitte, P., Die Zelle in der Evolution des Lebens. In *Studium generale: Auf dem Weg zu einem allgemeinen Teil der Wissenschaften*, Saner, L., Ed. Springer Fachmedien Wiesbaden: Wiesbaden, 2014; pp 137-146.
41. Smolen, V. F., Misconceptions and thermodynamic untenability of deviations from pH-partition hypothesis. *J. Pharm. Sci.* **1973,** *62* (1), 77-79.
42. Sugano, K.; Nabuchi, Y.; Machida, M.; Asoh, Y., Permeation characteristics of a hydrophilic basic compound across a bio-mimetic artificial membrane. *Int. J. Pharm.* **2004,** *275* (1-2), 271-278.
43. Takagi, M.; Taki, Y.; Sakane, T.; Nadai, T.; Sezaki, H.; Oku, N.; Yamashita, S., A new interpretation of salicylic acid transport across the lipid bilayer: implications of pH-dependent but not carrier-mediated absorption from the gastrointestinal tract. *J. Pharmacol. Exp. Ther.* **1998,** *285* (3), 1175-1180.
44. Teksin, Z. S.; Hom, K.; Balakrishnan, A.; Polli, J. E., Ion pair-mediated transport of metoprolol across a three lipid-component PAMPA system. *J Control Release* **2006,** *116* (1), 50-57.
45. Teorell, T., Transport processes in membranes in relation to the nerve mechanism. *Exp Cell Res* **1958,** *14* (Suppl 5), 83-100.
46. Tischbirek, C. H.; Wenzel, E. M.; Zheng, F.; Huth, T.; Amato, D.; Trapp, S.; Denker, A.; Welzel, O.; Lueke, K.; Svetlitchny, A.; Rauh, M.; Deusser, J.; Schwab, A.; Rizzoli, S. O.; Henkel, A. W.; Muller, C. P.; Alzheimer, C.; Kornhuber, J.; Groemer, T. W., Use-dependent inhibition of synaptic transmission by the secretion of intravesicularly accumulated antipsychotic drugs. *Neuron* **2012,** *74* (5), 830-844.
47. Trapp, S., Bioaccumulation of Polar and Ionizable Compounds in Plants. In *Ecotoxicology Modeling*, Devillers, J., Ed. Springer: Boston, MA, 2009; pp 299-353.
48. Trapp, S., Plant uptake and transport models for neutral and ionic chemicals. *Environ. Sci. Pollut. Res. Int.* **2004,** *11* (1), 33-39.
49. Trapp, S.; Franco, A.; Mackay, D., Activity-based concept for transport and partitioning of ionizing organics. *Environ. Sci. Technol.* **2010,** *44* (16), 6123-6129.
50. Trapp, S.; Horobin, R. W., A predictive model for the selective accumulation of chemicals in tumor cells. *Eur. Biophys. J.* **2005,** *34* (7), 959-966.
51. Trapp, S.; Rosania, G. R.; Horobin, R. W.; Kornhuber, J., Quantitative modeling of selective lysosomal targeting for drug design. *Eur. Biophys. J.* **2008,** *37* (8), 1317-1328.
52. Yang, Y.-Y.; Toor, G. S.; Williams, C. F., Pharmaceuticals and organochlorine pesticides in sediments of an urban river in Florida, USA. *J. of Soils and Sediments* **2015,** *15* (4), 993-1004.
53. Zheng, N.; Tsai, H. N.; Zhang, X.; Rosania, G. R., The Subcellular Distribution of Small Molecules: From Pharmacokinetics to Synthetic Biology. *Molecular Pharmaceutics* **2011,** *8* (5), 1619-1628.

Table 1. Physiochemical properties with compound abbreviation, molecular weight (MW), pK_a, log K_{ow} neutral and calculated log D at pH 5.5 and pH 7.0, input parameter for the model with calculated log K_{ow} ion and valency.

			chemical properties						model input	
	compound	**abbr.**	**MW** (g/mol)	**pK_a**[a] (base)	**pK_a**[a] (acid)	**log K_{ow} neutral**	**log D** (pH 5.5)	**log D** (pH 7.0)	**log K_{ow} ion**[b]	**Valency**[c]
neutral	Pymetrozine	PYME	217	4.1		-0.2	-0.2	-0.2	-3.7	1
	Thiamethoxam	THMX	292	-		-0.1	no pK_a	no pK_a	-3.6	1
	Cyantraniliprole	CYNT	474		9.1	1.9	1.9	1.9	-1.6	-1
	Carbamazepine	CBZ	236		13.9	2.3	2.3	2.3	-1.3	-1
	Spirotetramat	SPAT	373		10.7	2.5	2.5	2.5	-1.0	-1
acidic	Spirotetramat enol	SPAT enol	301		5.2	2.2	1.7	0.4	-1.3	-1
	Compound 1	compd 1	413		5.1	3.2	2.7	1.3	-0.3	-1
	Compound 2	compd 2	516		5.1	4.4	3.9	2.5	0.9	-1
basic	Compound 3	compd 3	272	9.4		0.3	-3.1	-2.1	-3.2	1
	Oxazoline	OX	220	8.7		2.3	-0.7	0.6	-1.2	1
	Compound 4	compd 4	211	9.1		2.4	-0.8	0.3	-1.1	1
	Compound 5	compd 5	235	9.6		2.6	-0.8	0.1	-0.9	1
	Compound 6	compd 6	237	9.6		3.3	-0.1	0.8	-0.2	1
	Imidazoline	IM	300	9.4		4.3	0.9	1.9	0.8	1
	Compound 7	compd 7	496	7.9		6.3	3.9	5.3	2.4	1
	Compound 8	compd 8	513	7.9		6.8	4.4	5.8	0.4	1

[a] pK_a values of PYME, THMX, CYNT, SPAT, SPAT enol, OX, IM were taken from Buchholz and Trapp (2016) [8]; CBZ was taken from Yang (2015) [52]; research compounds were taken from Syngenta internal data base

[b] log K_{ow} neutral = log K_{ow} ion + 3.5 from Trapp (2005) [50]

[c] z is the electric charge (synonym valency, for acids −, for bases +) [50]

Table 2. Kinetic and equilibrium measurements with the pH gradient conditions pH 7.0 to pH 5.5 and pH 5.5 to pH 7.0. P_e = effective permeability, M_d = Mass fraction in donor, M_a = Mass fraction in acceptor, ND = not determined, N/A = not analyzed (below limit of detection, LOD). Compounds with a difference between M_a and M_d of ≥ 15% were marked with "not equilibrated".

		pH 7.0 to pH 5.5			**pH 5.5 to pH 7.0**			
		kinetic	**equilibrium**		**kinetic**	**equilibrium**		
	compound	**P_e**	**M_a**	**M_r**	**P_e**	**M_d**	**M_r**	**comment**
		(10^{-6} cm/s)	**(%)**	**(%)**	**(10^{-6} cm/s)**	**(%)**	**(%)**	**equil. meas.**
neutral	Pymetrozine	0.19 ± 0.05	14 ± 2.2	0.0 ± 0.0	0.19 ± 0.01	78 ± 4.9	9.0 ± 4.9	not equilibrated
	Thiamethoxam	0.66 ± 0.13	28 ± 1.8	2.0 ± 1.8	0.65 ± 0.06	72 ± 2.3	1.0 ± 2.1	not equilibrated
	Cyantraniliprole	7.81 ± 1.06	42 ± 2.1	17 ± 5.1	7.41 ± 0.19	40 ± 1.2	22 ± 2.2	
	Carbamazepine	8.82 ± 1.11	N/A	N/A	8.55 ± 0.35	N/A	N/A	
	Spirotetramat	7.45 ± 1.34	26 ± 0.1	48 ± 1.4	11.45 ± 1.05	27 ± 0.6	50 ± 1.2	
acidic	Spirotetramat enol	0.05 ± 0.01	2.0 ± 1.6	4.0 ± 1.5	1.30 ± 0.03	61 ± 5.0	2.0 ± 4.0	not equilibrated
	Compound 1	0.18 ± 0.03	6.0 ± 1.7	0.0 ± 0.0	7.22 ± 0.25	10 ± 0.3	16 ± 0.9	
	Compound 2	0.43 ± 0.05	2.0 ± 2.9	56 ± 4.2	23.20 ± 1.81	2.0 ± 0.1	64 ± 0.7	
basic	Compound 3	0.06 ± 0.01	8.0 ± 8.8	16 ± 7.2	0.05 ± 0.00	98 ± 3.1	1.0 ± 2.4	not equilibrated
	Oxazoline	17.94 ± 4.49	85 ± 0.6	11 ± 10.6	0.58 ± 0.09	89 ± 2.5	4.0 ± 3.2	
	Compound 4	9.58 ± 0.48	81 ± 0.6	12 ± 1.5	0.32 ± 0.02	93 ± 6.9	3.0 ± 4.2	
	Compound 5	8.54 ± 0.94	46 ± 0.6	4.0 ± 4.2	0.45 ± 0.12	100 ± 0.0	0.0 ± 0.0	not equilibrated
	Compound 6	9.55 ± 0.82	78 ± 0.5	17 ± 1.1	0.38 ± 0.02	89 ± 2.0	5.0 ± 4.0	
	Imidazoline	42.46 ± 4.38	52 ± 0.2	45 ± 0.6	0.42 ± 0.07	62 ± 9.8	35 ± 10.2	
	Compound 7	N/A	2.0 ± 0.0	98 ± 2.9	N/A	3.0 ± 0.4	97 ± 0.4	
	Compound 8	N/A	ND	ND	N/A	0.0 ± 0.0	100 ± 0.0	

Table 3. Calculated membrane retention ('at lipid' fractions of cytosol and vacuole) and mass fractions of aqueous phases in four compartments (solved fraction of phloem, xylem, cytosol and vacuole). The amount of compound solved in vacuoles in relation to the overall dissolved fractions is denoted in brackets. Log K_{OW} of neutral species is given.

			'at lipids' (vac + cyt)	solved fractions (aqueous phases of given compartment)			
	compound	**log K_{ow}**	**$\%M_r$**	**$\%M_{phloem}$**	**$\%M_{xylem}$**	**$\%M_{cytosol}$**	**$\%M_{vacuole}$**
neutral	Pymetrozine	-0.2	3.3	2.2	2.8	9.6	82.1 (85%)
	Thiamethoxam	-0.1	4.3	2.3	2.8	10.1	80.5 (84%)
	Cyantraniliprole	1.9	84.0	0.4	0.5	1.7	13.4 (84%)
	Carbamazepine	2.3	91.5	0.2	0.2	0.9	7.1 (85%)
	Spirotetramat	2.5	95.2	0.1	0.1	0.5	4.1 (85%)
acidic	Spirotetramat enol	2.2	18.2	43.0	0.2	31.8	6.9 (8%)
	Compound 1	3.2	67.4	16.7	0.1	13.1	2.7 (8%)
	Compound 2	4.4	97.3	1.2	0.0	1.3	0.3 (11%)
basic	Compound 3	0.3	0.0	0.0	0.9	1.1	98 (98%)
	Oxazoline	2.3	1.1	0.0	1.1	0.4	97.3 (98%)
	Compound 4	2.4	0.9	0.0	0.9	0.7	97.6 (98%)
	Compound 5	2.6	1.0	0.1	0.7	1.6	96.7 (98%)
	Compound 6	3.3	5.3	0.1	0.3	1.5	92.8 (98%)
	Imidazoline	4.3	35.1	0.0	0.0	0.7	64.1 (99%)
	Compound 7	6.3	99.7	0.0	0.0	0.0	0.3 (100%)
	Compound 8	6.8	99.9	0.0	0.0	0.0	0.1 (100%)

Figure 1. Structures of tested agrochemicals, drugs and research compounds.

Figure 2. Schematic illustration of the compound diffusion from the donor to the acceptor compartment (Volume 50:50) in a pH gradient with buffer A and buffer B.

Figure 3. Effective permeabilities (P_e) measured from pH 7.0 to pH 5.5 and pH 5.5 to pH 7.0 in the kinetic PAMPA approach (18 h). The error bars represent the standard sample deviation.

Figure 4. Correlation between the difference of log D between donor and acceptor compartment (Δ log D) and the difference of log P_e from pH 5.5 to pH 7.0 and *vice versa* (Δ log P_e) measured in the kinetic approach.

Figure 5. Figure 5. Mass fractions of the aqueous phase in the acidic compartment (pH 5.5) after thermodynamic equilibration. This means the mass fractions are given without the membrane retention (see Equation 3) in donor ($M_{d,aq}$) and acceptor ($M_{a,aq}$) in pH gradient direction from pH 5.5 to pH 7.0 and pH 7.0 to pH 5.5, respectively. The dotted lines represent the average mass fraction of compound species in the acidic compartment: neutral 51%, acidic 15% and basic 86%. Not equilibrated compounds are marked with an asterisk. The error bars represent the standard sample deviation.

Figure 6. Mass fractions at equilibrium for donor (M_d), acceptor (M_a) and membrane retention (M_r). (A) Mass fractions calculated with the 'PAMPA cell model'. (B) Mass distributions measured with PAMPA (see Method).

Figure 7. Impact of log K_{ow} and pK_a on mass distributions in 'at lipids' and in solved fractions (Table 3). (A) Correlation between log K_{ow} and membrane retention related to compound species. The dotted lines represent the membrane retention tendency for each compound species. (B) Correlation between log K_{ow} and mass fraction in vacuoles relative to total aqueous phase for each compound species. The dotted lines represent the average for each compound species.

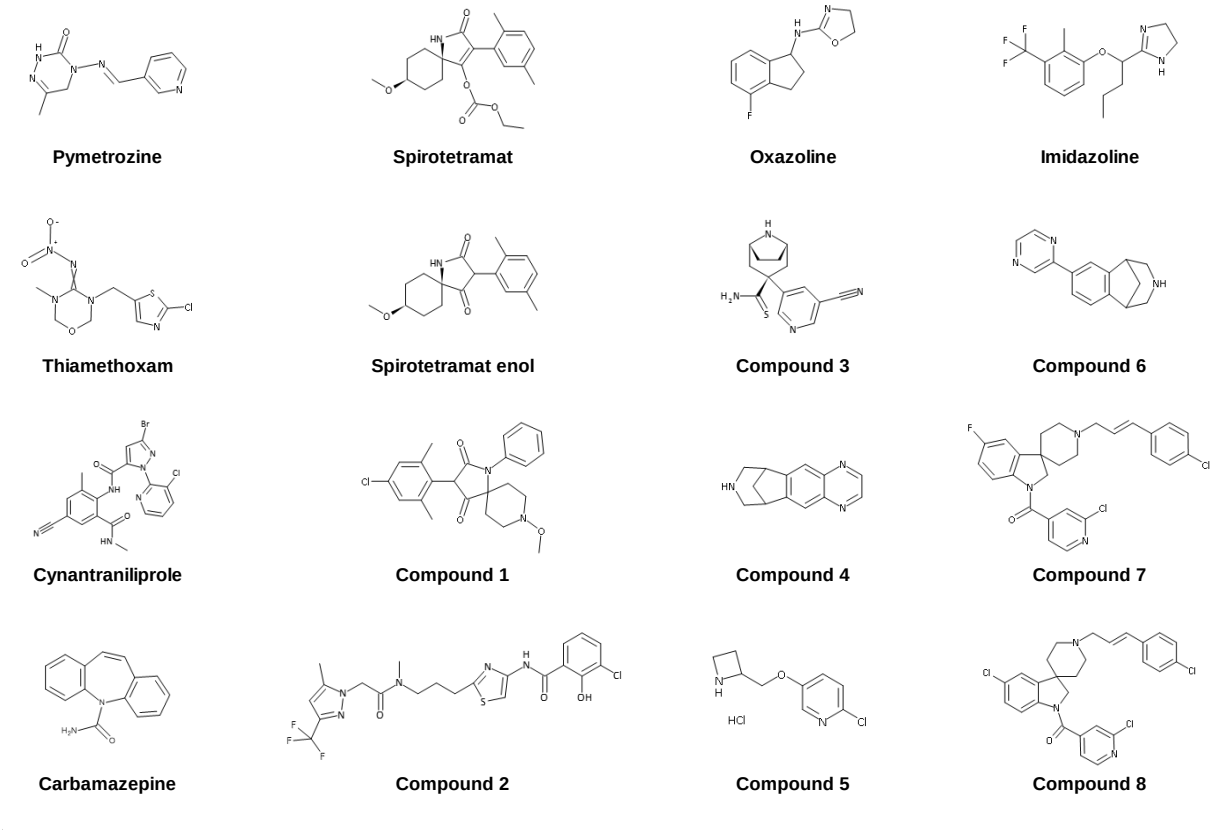
Pymetrozine
Spirotetramat
Oxazoline
Imidazoline
Thiamethoxam
Spirotetramat enol
Compound 3
Compound 6
Cynantraniliprole
Compound 1
Compound 4
Compound 7
Carbamazepine
Compound 2
Compound 5
Compound 8

Figure 1.

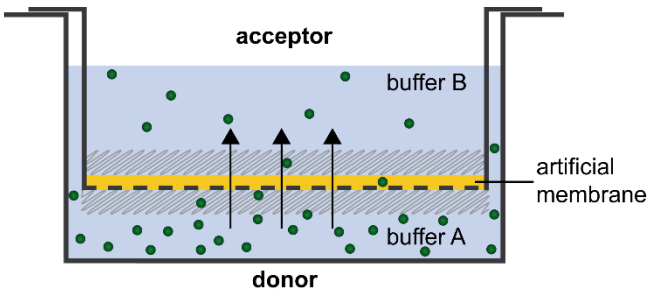

Figure 2.

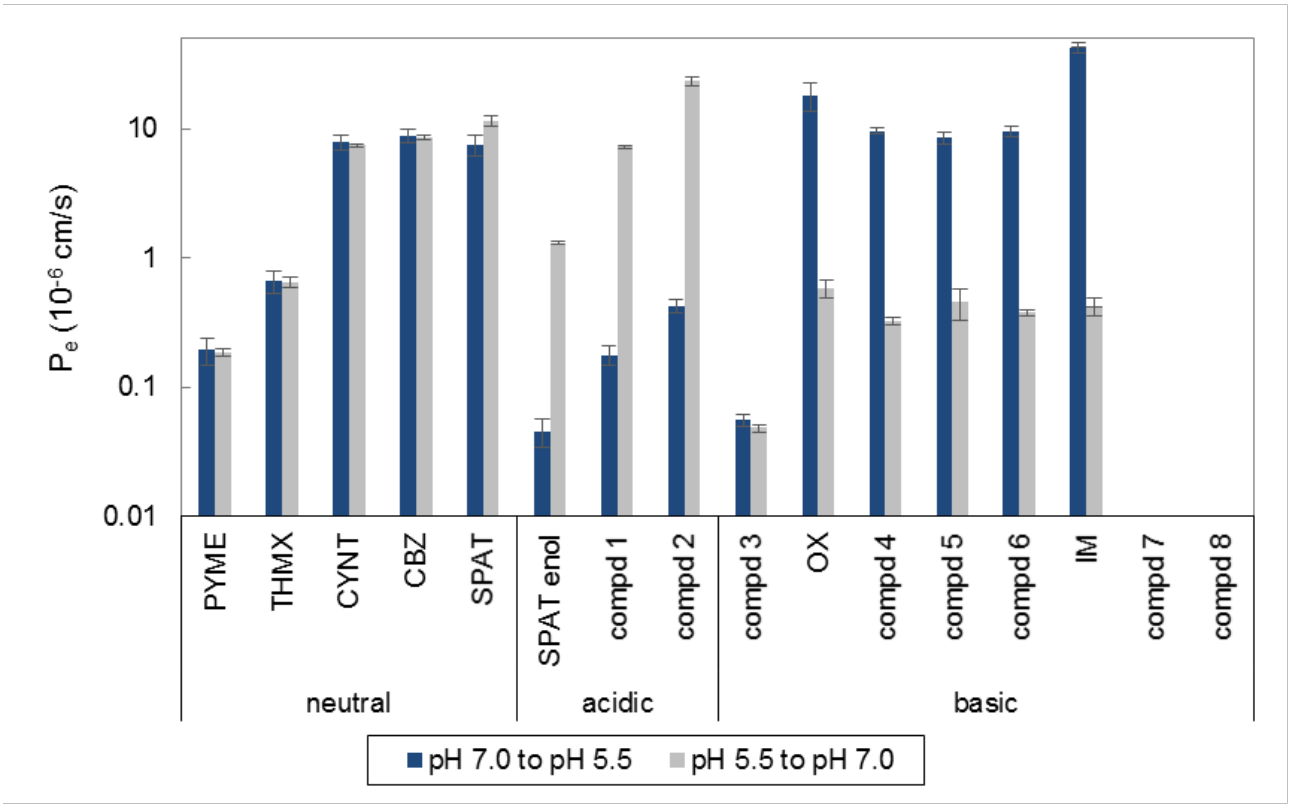
10
1
0.1
0.01
P_e (10^{-6} cm/s)
PYME
THMX
CYNT
CBZ
SPAT
SPAT enol
compd 1
compd 2
compd 3
OX
compd 4
compd 5
compd 6
IM
compd 7
compd 8
neutral
acidic
basic
pH 7.0 to pH 5.5
pH 5.5 to pH 7.0

Figure 3.

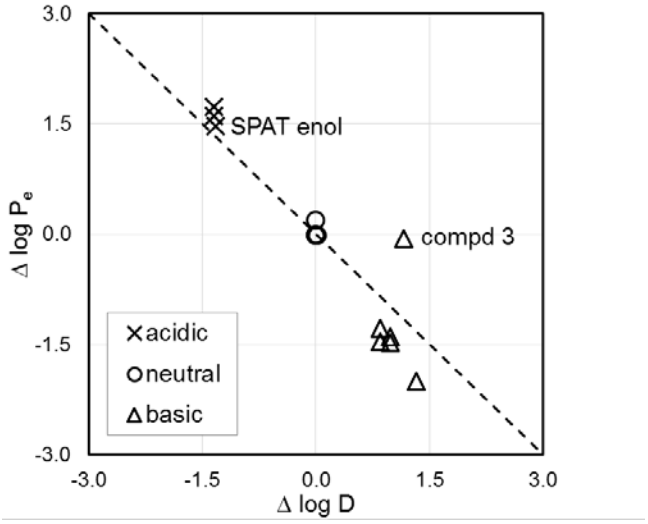
3.0
1.5
0.0
-1.5
-3.0
Δ log Pe
-3.0
-1.5
0.0
1.5
3.0
Δ log D
SPAT enol
Δ compd 3
×acidic
○neutral
Δbasic

Figure 4.

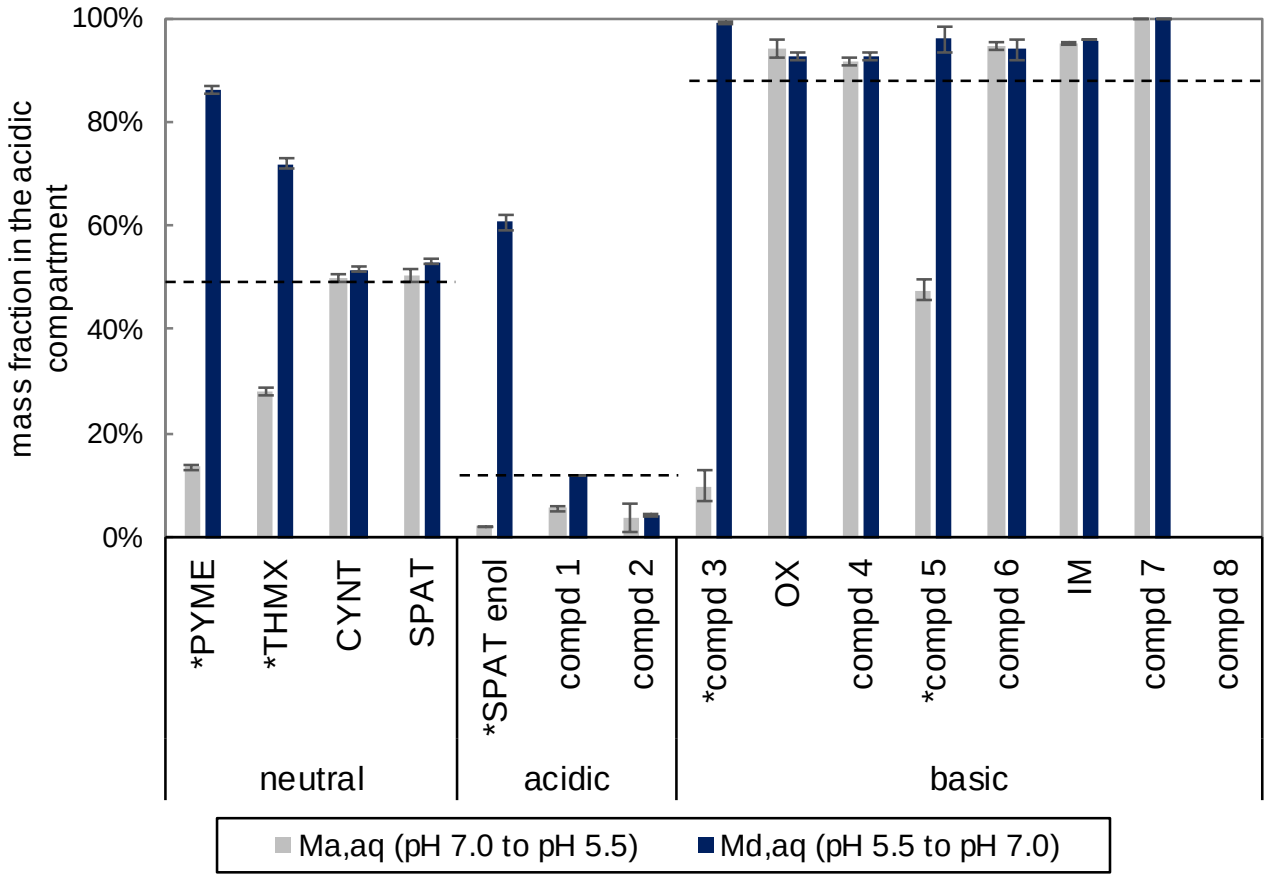
100%
80%
60%
40%
20%
0%
mass fraction in the acidic compartment
*PYME
*THMX
CYNT
SPAT
*SPAT enol
compd 1
compd 2
*compd 3
OX
compd 4
*compd 5
compd 6
IM
compd 7
compd 8
neutral
acidic
basic
Ma,aq (pH 7.0 to pH 5.5)
Md,aq (pH 5.5 to pH 7.0)

Figure 5.

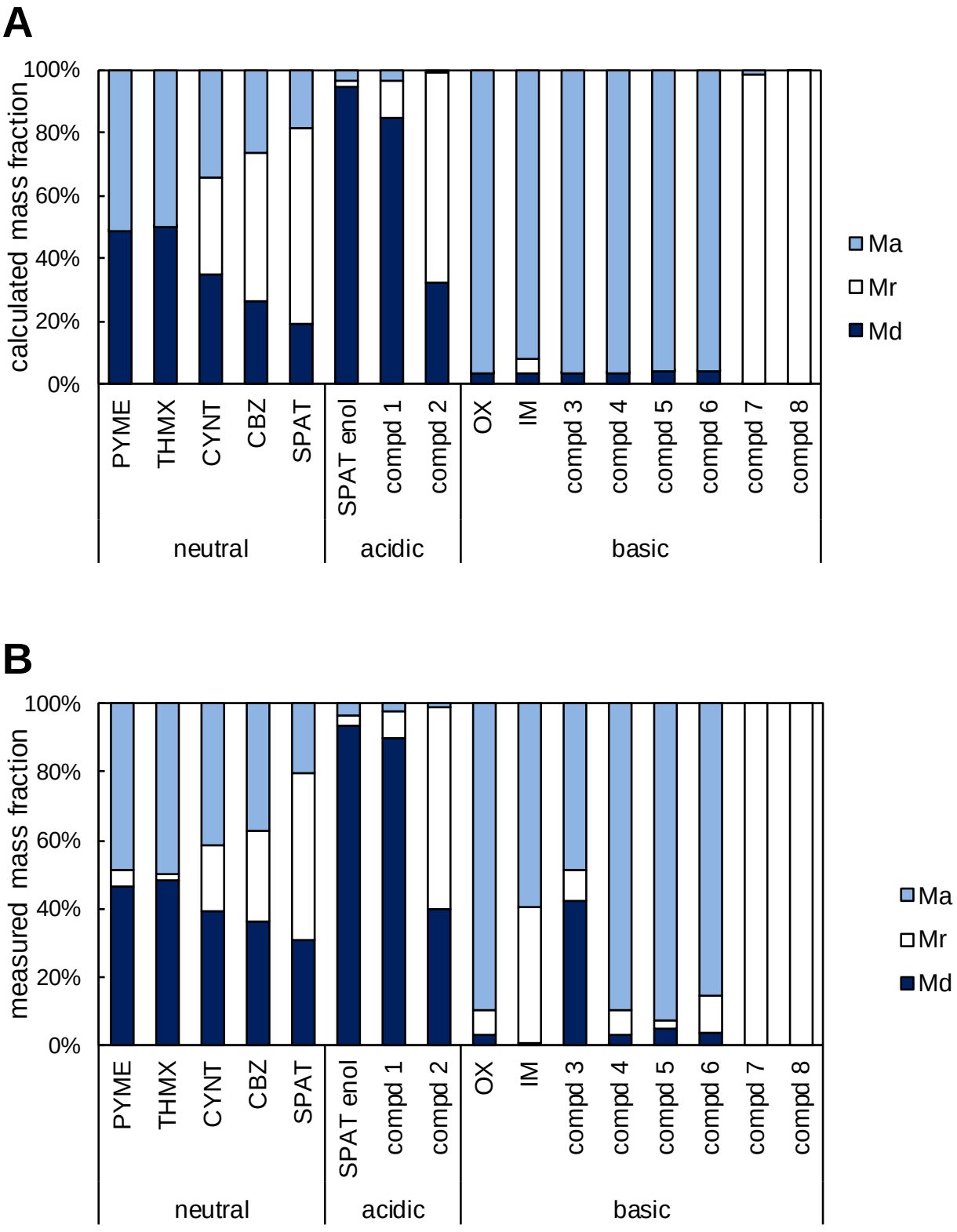
A
calculated mass fraction
100%
80%
60%
40%
20%
0%
PYME
THMX
CYNT
CBZ
SPAT
SPAT enol
compd 1
compd 2
OX
IM
compd 3
compd 4
compd 5
compd 6
compd 7
compd 8
neutral
acidic
basic
Ma
Mr
Md
B
measured mass fraction
100%
80%
60%
40%
20%
0%
PYME
THMX
CYNT
CBZ
SPAT
SPAT enol
compd 1
compd 2
OX
IM
compd 3
compd 4
compd 5
compd 6
compd 7
compd 8
neutral
acidic
basic
Ma
Mr
Md

Figure 6.

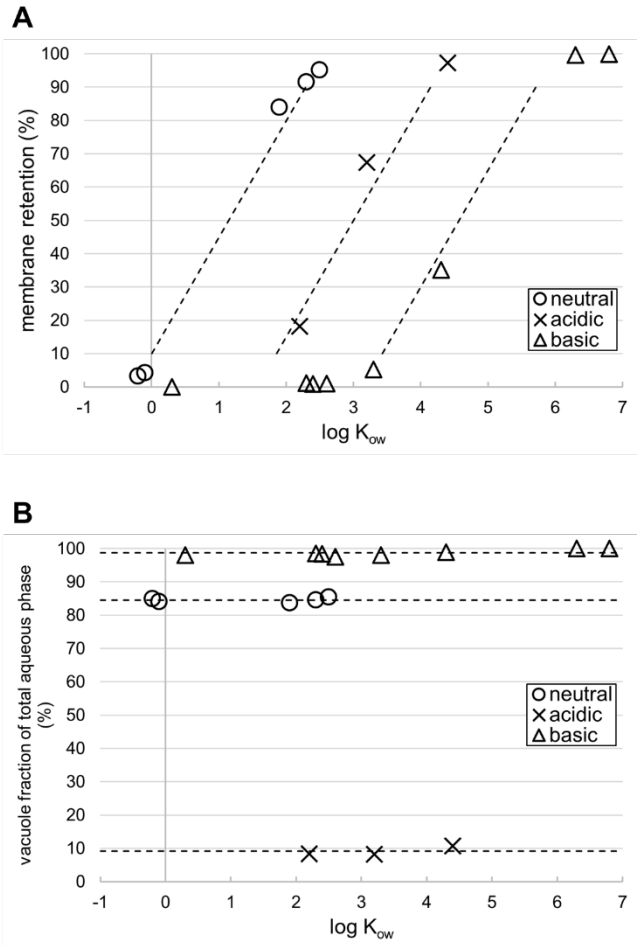

654

655 **Figure 7.**

656

657 **Table of Contents graphic**

658

659 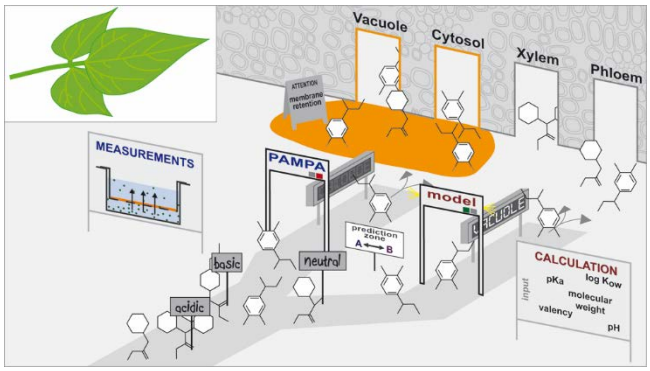

660

661